Bcl-x_L gain of function and p19^{ARF} loss of function cooperate oncogenically with Myc in vivo by distinct mechanisms

Andrew Finch,[1] Julia Prescott,[2] Ksenya Shchors,[1] Abigail Hunt,[1] Laura Soucek,[1] Tobias B. Dansen,[3] Lamorna Brown Swigart,[1] and Gerard I. Evan[1,*]

[1] Cancer Research Institute and Department of Cellular and Molecular Pharmacology, UCSF Comprehensive Cancer Center, 2340 Sutter Street, San Francisco, California 94143
[2] Present address: Pharmacyclics Inc., 995 East Arques Avenue, Sunnyvale, California 94805.
[3] Present address: UMC Utrecht, Department of Physiological Chemistry, Universiteitsweg 100, 3584 CG Utrecht, Netherlands.
*Correspondence: gevan@cc.ucsf.edu

Summary

Overexpression of Bcl-x_L, loss of p19^{ARF}, and loss of p53 all accelerate Myc oncogenesis. All three lesions are implicated in suppressing Myc-induced apoptosis, suggesting that this is a common mechanism by which they synergize with Myc. However, using an acutely switchable model of Myc-induced tumorigenesis, we demonstrate that each lesion cooperates with Myc in vivo by a distinct mechanism. While Bcl-x_L blocks Myc-induced apoptosis, inactivation of p19^{ARF} enhances it. However, this increase in apoptosis is matched by increased Myc-induced proliferation. p53 inactivation shares features of both lesions, partially suppressing apoptosis while augmenting proliferation. Bcl-x_L and p19^{ARF} loss together synergize to further accelerate Myc oncogenesis. Thus, differing lesions cooperate oncogenically with Myc by discrete mechanisms that can themselves synergize with each other.

Introduction

The tumorigenic consequences of oncogene activation are restrained by intrinsic tumor suppression pathways, of which the best characterized are induction of apoptosis and proliferative arrest (Evan and Vousden, 2001; Lowe et al., 2004). As a consequence, tumorigenesis can arise only as a result of multiple, complementary oncogenic lesions that cooperate to defuse the intrinsic tumor suppressor pathways triggered by each other. For this reason, individual oncogenic mutations are, typically, highly inefficient at driving tumorigenesis in individual somatic cells. The oncogene c-*myc* is a well-characterized example of this phenomenon. c-*myc* encodes a member of the basic-helix-loop-helix-leucine zipper transcription factor family, Myc, that coordinates expression of many diverse genes involved in processes necessary for cell expansion, including cell growth, metabolism, ribosome biogenesis, proliferation, and differentiation (Adhikary and Eilers, 2005; Hurlin and Dezfouli, 2004). This central role in cell expansion underlies the frequent selection for deregulation and/or overexpression of Myc in many human tumors. At the same time, aberrant Myc expression is also a powerful promoter of apoptosis, an intrinsic tumor suppressor mechanism that serves as a powerful inbuilt restraint to Myc's oncogenic action. By specifically gating the intrinsic apoptotic Myc tumor suppressor pathway, mutations that suppress apoptosis, such as overexpression of members of the antiapoptotic Bcl-2/Bcl-x_L family (Bissonnette et al., 1992; Fanidi et al., 1992; Pelengaris et al., 2002; Wagner et al., 1993), potently cooperate with Myc to drive tumorigenesis (Strasser et al., 1990).

As with many other dominant oncoproteins, activated Myc triggers p53 via the induction of the tumor suppressor *p19^{ARF}*. Loss of either p19^{ARF} (Eischen et al., 1999; Schmitt et al., 1999) or p53 (Elson et al., 1995; Hsu et al., 1995), like overexpression of Bcl-2, greatly accelerates Myc oncogenesis in a wide variety of transgenic mouse tumor models. Several studies suggest that loss of either p19^{ARF} (Zindy et al., 1998) or p53 (Hermeking and Eick, 1994; Wagner et al., 1994) suppresses Myc-induced apoptosis in fibroblasts in vitro, although such studies are complicated by the need for serum deprivation to trigger such Myc-dependent apoptosis because withdrawal of serum, a potent cocktail of inflammatory mitogens and survival factors, is a powerful promoter of both proliferative arrest and cell death in its own right. More recently, studies using transgenic and transplanted Myc-induced lymphoma models have

SIGNIFICANCE

Apoptosis is a crucial intrinsic tumor suppressor mechanism that limits Myc's oncogenic potential. Here, we ask whether all oncogenic lesions that cooperate with Myc in vivo do so by suppressing apoptosis. We show that Bcl-x_L overexpression, loss of p19^{ARF}, and loss of p53 each cooperate with Myc by a distinct mechanism. Bcl-x_L blocks apoptosis, whereas inactivation of p19^{ARF} enhances both Myc-induced apoptosis and Myc-induced proliferation, generating a tissue with roughly normal cell numbers but greatly increased cell turnover. p53 augments Myc-induced proliferation but also affords partial protection from apoptosis, thus establishing a highly aggressive tumor phenotype. Thus, oncogenes cooperate by discrete mechanisms, suggesting that there are multiple ways by which the balance between cell gain and cell loss might be reestablished therapeutically in tumors.

indicated that inactivation of apoptosis through overexpression of Bcl-2 or loss of Bax relieves selective pressures to lose p53 function during lymphomagenesis (Eischen et al., 2001; Schmitt et al., 2002), again hinting that p53 functions to mediate Myc-induced apoptosis in such models. On the other hand, there are many known instances where a functional $p19^{ARF}$/p53 pathway is not required for Myc-induced apoptosis. For example, Myc-induced apoptosis is independent of p53 in Myc-induced lymphoma (Hsu et al., 1995), as is Myc-dependent apoptosis (Lenahan and Ozer, 1996) and release of mitochondrial holocytochrome c (Juin et al., 1999) in fibroblasts in vitro, intimating that loss of p53 would offer no protection from apoptosis in such instances. The role of $p19^{ARF}$ in Myc-induced apoptosis is even less clear, given that inactivation of apoptosis through Bax loss fails to relieve any pressure on loss of $p19^{ARF}$ function during lymphomagenesis (Eischen et al., 2001). Together, such observations suggest that loss of $p19^{ARF}$ and/or p53 may promote Myc-induced tumorigenesis by mechanisms other than apoptosis suppression. Since both $p19^{ARF}$ (Kamijo et al., 1998; Kuo et al., 2003) and p53 (Lowe et al., 2004) exert profound antiproliferative influences, one plausible possibility is that loss of $p19^{ARF}$ and/or p53 serves to abrogate an intrinsic antiproliferative pathway triggered by Myc activation.

Classical transgenic and knockout mouse tumor models possess constitutively preconfigured genetic backgrounds that predispose them to neoplasia, but they rely on sporadic, uncontrolled, and largely unknown secondary lesions to precipitate the actual onset and progression of tumors. Many studies indicate that combining different, hardwired transgenic or knockout lesions can accelerate or retard tumorigenesis. However, the rarity of the eventual clonal tumors that emerge among all the target somatic cells, the extended time over which they do so, and the arcane nature of the additional sporadic lesions that are required all mean that it is not possible to infer back from tumor incidence studies how such hardwired lesions interacted in the normal cells from which the tumor evolved. To circumvent this problem, we have employed a reversibly switchable model of Myc oncogenesis in which the timing of the initial Myc activation event is precisely known and controlled within the target tissue. This allows real-time monitoring of the interaction between Myc and any other oncogenic lesions during the earliest stages of tumor initiation through progression and into tumor maintenance. Here, we use a version of this switchable model of Myc-induced oncogenesis in β cells (Pelengaris et al., 2002) to compare directly the impact of an antiapoptotic lesion, Bcl-x_L, and inactivation of either $p19^{ARF}$ or p53 in modulating the capacity of Myc to initiate and drive tumorigenesis in vivo.

Results

Bcl-x_L expression, ARF loss, and p53 loss each elicit a distinct outcome following Myc activation in pancreatic β cells

In *pIns-MycER^{TAM}* mice, expression of the acutely and reversibly switchable MycER^{TAM} protein is driven specifically in pancreatic β cells from the mouse insulin promoter. As previously described (Pelengaris et al., 2002), acute activation of Myc in *pIns-MycER^{TAM}* mice induces rapid onset of both proliferation and apoptosis, the latter overwhelming the former and leading to rapid β cell depletion (Pelengaris et al., 2002). Coexpression of the apoptosis suppressor Bcl-x_L in β cells efficiently blocks Myc-induced β cell apoptosis, and as a consequence, sustained Myc activation in such *pIns-MycER^{TAM};RIP7-Bcl-x_L* mice drives progressive β cell expansion synchronously in all pancreatic islets. Such expansion is concomitant with progressive acquisition of classical attributes of tumorigenesis, including dedifferentiation, tissue dysplasia and remodeling, angiogenesis, local invasion, and metastasis (Pelengaris et al., 2002). Hence, suppression of the intrinsic Myc-driven apoptotic program is sufficient to expose the oncoprotein's multifarious tumorigenic potential.

Many studies have implicated the p53 pathway in mediation of Myc-induced apoptosis. The critical conduit by which oncogenic Myc activates p53 is the tumor suppressor $p19^{ARF}$ (Zindy et al., 1998) and, consistent with this, inactivation or loss of $p19^{ARF}$ or p53 exhibits dramatic oncogenic synergy with Myc (Eischen et al., 1999; Schmitt et al., 1999). To assess whether, and how, loss of either *ARF* or *p53* synergizes oncogenically with Myc in our switchable β cell model, we activated MycER^{TAM} in β cells of *ARF*$^{-/-}$ or *p53*$^{-/-}$ mice and examined β cell dynamics in each case, using BrdU incorporation to assess β cell proliferation and TUNEL staining to monitor apoptosis. As described, activation of Myc for 3 days in *pIns-MycER^{TAM}* β cells induces both apoptosis and proliferation (Figures 1A and 1E), while Bcl-x_L overexpression in the *pIns-MycER^{TAM};RIP7-Bcl-x_L* bitransgenic mice blocks Myc-induced apoptosis (Figure 1B) but allows proliferation to drive net β cell expansion (Figure 1F). Thus, Bcl-x_L cooperates with Myc by selectively blocking the intrinsic apoptotic tumor suppressor function of Myc. By contrast, analogous analysis of proliferation and apoptosis in *ARF*$^{-/-}$ β cells following Myc activation revealed no measurable suppression of apoptosis compared with that in *ARF^{wt}* controls (Figure 1C). Indeed, TUNEL staining indicated a 2.5-fold increase in apoptosis at 72 hr post-Myc activation in *ARF*$^{-/-}$ β cells (9.9% apoptosis in *pIns-MycER^{TAM}* mice versus 25.2% in *pIns-MycER^{TAM};ARF*$^{-/-}$ mice). However, this increased apoptosis was accompanied by a marked increase in β cell proliferation over that in *ARF^{wt}* or Bcl-x_L-overexpressing β cells (Figure 1G): at 72 hr after Myc activation BrdU incorporation was ~3-fold higher in the absence of *ARF* (3.3% ± 0.06% in *pIns-MycER^{TAM}* mice, 4.9% ± 1.85% in *pIns-MycER^{TAM};RIP7-Bcl-x_L* mice, and 10.2% ± 1.08% in *pIns-MycER^{TAM};ARF*$^{-/-}$ mice). Activation of Myc in *p53*$^{-/-}$ β cells also induced apoptosis, although this was partially suppressed compared with β cells from *pIns-MycER^{TAM}* mice (from 9.9% down to 5.6%; Figure 1D). Analysis of BrdU incorporation revealed that p53 loss augmented Myc-induced β cell proliferation relative to that in *pIns-MycER^{TAM};RIP7-Bcl-x_L* β cells, to a degree similar to that seen in the absence of $p19^{ARF}$ (Figure 1H; BrdU incorporation of 13.6% ± 4.1%), consistent with the antiproliferative effects of $p19^{ARF}$ being, in great part, p53 dependent.

The enhancement of Myc-induced β cell proliferation conferred by *ARF* loss is not due to increased expression of the *MycER^{TAM}* transgene

Activity of the insulin promoter element used to drive expression of MycER^{TAM} in the *pIns-MycER^{TAM}* model is potentially sensitive to the differentiation status of β cells (Pelengaris et al., 2002). Since Myc is known to suppress differentiation in many cell lineages, we needed to confirm that the changes we observe in Myc-driven proliferation in various genetic backgrounds are not merely a trivial consequence of suppression of *insulin*

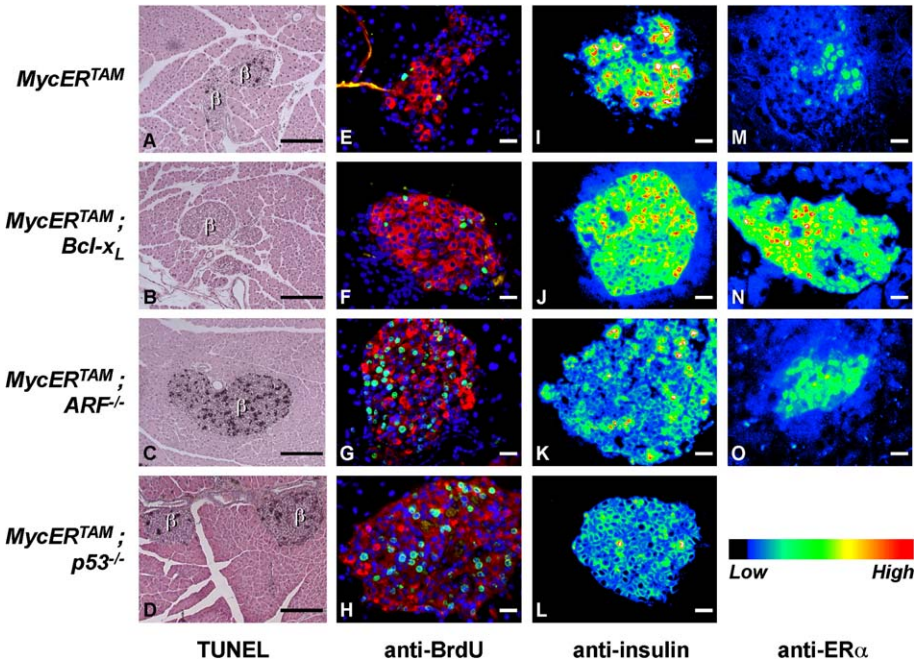

Figure 1. Bcl-x_L overexpression, p19^{ARF} loss, and p53 loss each modulate Myc's oncogenic potential by distinct mechanisms

Myc was activated in β cells of pancreatic islets of *pIns-MycER^{TAM}* (**A**, **E**, **I**, and **M**), *pIns-MycER^{TAM};RIP7-Bcl-x_L* (**B**, **F**, **J**, and **N**), *pIns-MycER^{TAM};ARF$^{-/-}$* (**C**, **G**, **K**, and **O**), or *pIns-MycER^{TAM};p53$^{-/-}$* (**D**, **H**, and **L**) mice for 3 days. 3.5 hr prior to sacrifice, BrdU was administered systemically. Pancreas sections were stained for apoptosis by TUNEL (gray with eosin counterstain) (**A**–**D**), with anti-BrdU (green) plus anti-insulin (red) and Hoechst (blue) counterstain (**E**–**H**) to identify S phase β cells, or with anti-insulin (**I**–**L**) or anti-ERα (**M**–**O**) followed by excess fluorescent secondary antibody to allow quantitative imaging. A quantitative color scale is shown below **O**. "β" denotes islets. Scale bars are 100 μm (**A**–**D**) and 20 μm (**E**–**O**). The occasional bright punctate fluorescent staining seen in the anti-insulin-stained sections correlates with apoptotic cells and is evident in islets from all but the *pIns-MycER^{TAM};RIP7-Bcl-x_L* mice.

promoter-driven MycER^{TAM} expression. To address this, tissue sections were stained with anti-insulin antibody and insulin expression levels assayed by quantitative immunofluorescence. After 3 days Myc activation, insulin expression was comparable in *pIns-MycER^{TAM}* mice and in *pIns-MycER^{TAM};RIP7-Bcl-x_L* bitransgenic mice (Figures 1I and 1J) and somewhat decreased in β cells of *pIns-MycER^{TAM};ARF$^{-/-}$* and *pIns-MycER^{TAM};p53$^{-/-}$* mice (Figures 1K and 1L). Given the inverse relationship between Myc-induced proliferation and terminal differentiation in β cells (Laybutt et al., 2002), as in many other cell lineages, this decrease in insulin staining is consistent with the increased proliferation that we observe in *ARF$^{-/-}$* and *p53$^{-/-}$* β cells. Since the insulin promoter drives expression of the MycER^{TAM} transgene, these data suggest that expression of MycER^{TAM} is, if anything, lower in *ARF$^{-/-}$* and *p53$^{-/-}$* mice than in *pIns-MycER^{TAM};RIP7-Bcl-x_L* animals.

We used quantitative immunofluorescence analysis of ERα immunoreactivity to ascertain directly levels of MycER^{TAM} in β cells. This showed that expression of MycER^{TAM} was roughly equivalent in the *ARF^{wt}* and *ARF$^{-/-}$* backgrounds (Figures 1M and 1O), both of which were significantly less than in *pIns-MycER^{TAM};RIP7-Bcl-x_L* β cells (Figure 1N). This is despite the fact that Myc-induced β cell proliferation is markedly lower in *pIns-MycER^{TAM};RIP7-Bcl-x_L* β cells than in β cells of *ARF$^{-/-}$* mice. No ERα immunoreactivity was observed in nontransgenic islets (data not shown). While decreased expression of the *insulin* promoter-driven *MycER^{TAM}* transgene in *ARF$^{-/-}$* β cells relative to their *pIns-MycER^{TAM};RIP7-Bcl-x_L* counterparts may be a consequence of their increased proliferation and concomitantly depressed terminal differentiation, it is also possible that β cells expressing high levels of MycER^{TAM} are preferentially eradicated by apoptosis in *ARF$^{-/-}$* animals, whereas such selective culling is blocked in *pIns-MycER^{TAM};RIP7-Bcl-x_L* β cells. Whatever the explanation, however, it is clear that the enhanced Myc-induced proliferation observed in *ARF$^{-/-}$* β cells is not due to elevated MycER^{TAM} expression: indeed, it occurs despite significant MycER^{TAM} downregulation in p19^{ARF}-deficient β cells.

Enhanced Myc-induced proliferation in β cells lacking p19^{ARF} or p53 correlates with a failure of Myc to induce p21^{cip1}

Myc is a potent inducer of the cell cycle inhibitor p21^{cip1}. This induction requires both ARF and p53 (Zindy et al., 1998), providing a potential mechanism for the enhanced proliferation afforded by Myc in *ARF*- and *p53*-deficient β cells. We therefore assayed the expression of p19^{ARF}, p53, and p21^{cip1} following Myc activation in β cells in vivo by immunofluorescence. Activation of Myc strongly induced p19^{ARF} in both *pIns-MycER^{TAM}* mice (Figures 2A and 2B) and *pIns-MycER^{TAM};RIP7-Bcl-x_L* mice (data not shown). Myc also induced accumulation of p53 (Figures 2C and 2D), although much of this appeared to be p19^{ARF} independent (Figures 2E and 2F). Both p19^{ARF} upregulation and p53 stabilization were accompanied by strong induction of nuclear p21^{cip1} (Figures 2G and 2H). By contrast, in both *pIns-MycER^{TAM};ARF$^{-/-}$* and *pIns-MycER^{TAM};p53$^{-/-}$* mice, induction of p21^{cip1} by Myc was strongly suppressed (Figures 2I and 2J). Thus, the enhanced pro-proliferative activity of Myc in p19^{ARF}- and p53-deficient β cells correlates with a failure of Myc to induce p21^{cip1} in these genetic backgrounds.

Bcl-x_L overexpression and p19^{ARF} loss synergize with each other to augment Myc's oncogenic activity

Our data demonstrate that gain of function in Bcl-x_L and loss of p19^{ARF} function cooperate oncogenically with Myc in β cells in vivo by fundamentally distinct mechanisms: Bcl-x_L specifically blocks Myc-induced apoptosis while permitting Myc-induced proliferation, whereas loss of p19^{ARF} augments Myc-induced proliferation, possibly through disruption of the p53/p21^{cip1} axis, to the extent that it balances or exceeds cell loss through apoptosis. One prediction from these observations is

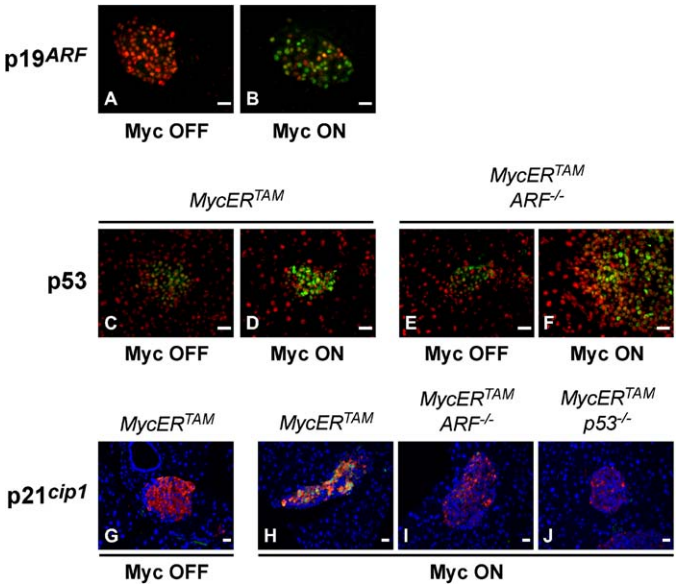

Figure 2. Myc-dependent induction of p21^{cip1} requires functional p19^{ARF} and p53

Sections from 1 day (**A** and **B**) or 3 day (**C**–**J**) islets from control oil (Myc OFF)- or tamoxifen (Myc ON)-treated *pIns-MycER^{TAM}* (**A**–**D**, **G**, and **H**), *pIns-MycER^{TAM};ARF$^{-/-}$* (**E**, **F**, and **I**), or *pIns-MycER^{TAM};p53$^{-/-}$* mice (**J**) were stained with anti-p19^{ARF} antibody (green) plus anti-ER counterstain (red) (**A** and **B**), anti-p53 antibody (green) (**C**–**F**), or anti-p21 antibody (green) with insulin counterstain (red) (**G**–**J**). Myc activation induces upregulation of p19^{ARF} and p21. The upregulation of p21^{cip1} is dependent upon the presence of p19^{ARF} and p53. Occasional nonnuclear green staining (**H**–**J**) is due to tissue autofluorescence. Scale bars are 20 μm (**A**–**F**) and 10 μm (**G**–**J**).

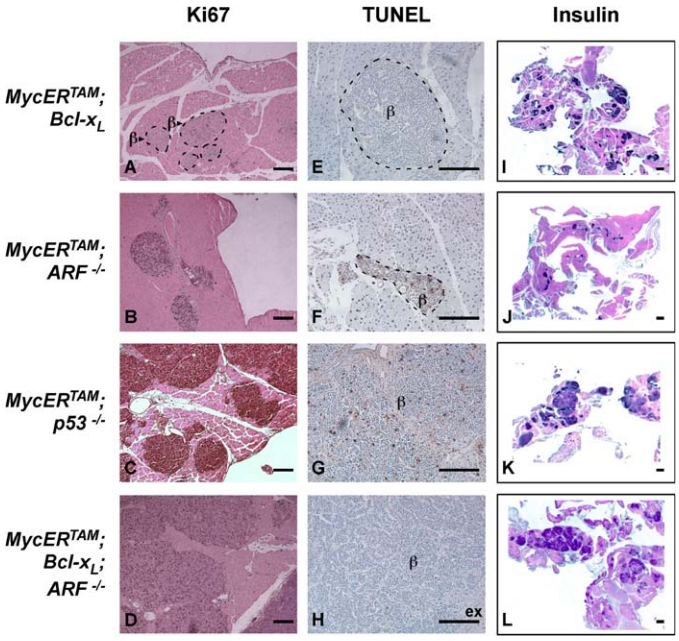

Figure 3. Bcl-x$_L$ overexpression, loss of p19^{ARF}, and loss of p53 each synergize with Myc by discrete mechanisms to promote tumorigenesis

Myc was activated for 12 days in pancreatic β cells of *pIns-MycER^{TAM};RIP7-Bcl-x$_L$* (**A**, **E**, and **I**), *pIns-MycER^{TAM};ARF$^{-/-}$* (**B**, **F**, and **J**), *pIns-MycER^{TAM};p53$^{-/-}$* (**C**, **G**, and **K**), or *pIns-MycER^{TAM};*RIP7*-Bcl-x$_L$;ARF$^{-/-}$* (**D**, **H**, and **L**) mice. Pancreas sections were stained with anti-Ki67 (**A**–**D**, dark brown with eosin counterstain), by TUNEL (**E**–**H**, brown with hematoxylin counterstain) or anti-insulin (gray/blue with eosin counterstain [**I**–**L**]). Examples of islets are indicated by "β." Scale bars are 20 μm (**A**–**H**) and 500 μm (**I**–**L**). ex, exocrine tissue.

that the combination of both Bcl-x$_L$ overexpression and p19^{ARF} loss together should greatly accelerate Myc-induced tumorigenesis over either one alone. To test this directly, we crossed the *pIns-MycER^{TAM};RIP7-Bcl-x$_L$* mice onto our *ARF*-deficient background and activated MycER^{TAM} in β cells for 12 days to induce tumor formation. First, we assessed whether the two lesions could indeed synergistically cooperate with Myc activation. Ki67 staining and TUNEL analysis revealed that the mechanistic differences between Bcl-x$_L$ overexpression and p19^{ARF} loss that we observed after 3 days of sustained Myc activation (Figure 1) are maintained at the later times (12 days). Thus, β cells from the *pIns-MycER^{TAM};RIP7-Bcl-x$_L$* mice exhibit relatively modest Myc-dependent proliferation combined with a complete absence of apoptosis (Figures 3A and 3E), while β cells from *pIns-MycER^{TAM}/ARF$^{-/-}$* mice exhibit a high proliferative rate together with high apoptosis (Figures 3B and 3F). β cells from *pIns-MycER^{TAM}/p53$^{-/-}$* mice also behaved as expected, exhibiting a high proliferative rate with partial incomplete suppression of apoptosis (Figures 3C and 3G). As predicted, β cells from the *pIns-MycER^{TAM};RIP7-Bcl-x$_L$;ARF$^{-/-}$* mice combined the features of each separate cooperating mutation, exhibiting complete absence of apoptosis together with a high rate of proliferation (Figures 3D and 3H).

To assess the influence of the differing cooperating lesions on overt Myc-induced β cell tumorigenesis, we examined the histological characteristics of the 12 day β cell tumors in each case. As described previously (Pelengaris et al., 2002), 12 days of sustained Myc activation alone in *pIns-MycER^{TAM}* mice triggers involution of all islets due to overwhelming apoptosis of virtually all pancreatic β cell populations, resulting in diabetes. Suppression of Myc-induced apoptosis by coexpression of Bcl-x$_L$ exposes Myc's diverse oncogenic potential, driving expansion and tumorigenesis of each β cell population in each islet (Figure 3I). These mice develop transient diabetes (due to Myc-induced partial dedifferentiation and consequent reduction in insulin secretion), but their blood glucose subsequently returns to normal due to steady expansion of the β cell compartment (Pelengaris et al., 2002). In *ARF$^{-/-}$* mice, Myc-induced β cell apoptosis is more or less offset by the enhanced rate of Myc-induced proliferation, resulting in dramatically increased β cell turnover but little overall change in β cell mass over time (Figure 3J). This amalgam of Myc-induced dedifferentiation and lack of overall β cell expansion eventually leads to diabetes (a rise in blood glucose from 69 mg/dl ± 23 mg/dl prior to treatment to 324 mg/dl ± 158 mg/dl at day 12 after treatment). In *p53$^{-/-}$* animals, enhanced Myc-induced proliferation plus partial suppression of apoptosis drives a more rapid overall β cell expansion than that observed in Bcl-x$_L$-expressing mice (Figure 3K). In *pIns-MycER^{TAM};RIP7-Bcl-x$_L$;ARF$^{-/-}$* mice, the combination of enhanced proliferation together with abrogation of apoptosis promotes extremely rapid and progressive β cell tumorigenesis that is so extensive as to occupy the majority of the central portion of the pancreas after only 12 days (Figure 3L). Such mice remained free from diabetes throughout (blood glucose of 151 mg/dl ± 31 mg/dl, within the normal range for C57Bl6 mice), presumably because massive expansion of the β cell compartment compensates for their partial dedifferentiation.

By several criteria, Myc-induced tumorigenesis in the *pIns-MycER^{TAM};RIP7-Bcl-x$_L$;ARF$^{-/-}$* mice is far more severe than that in either *pIns-MycER^{TAM};RIP7-Bcl-x$_L$* or *pIns-MycER^{TAM};ARF$^{-/-}$* animals. Twelve day tumors induced by Myc in *pIns-MycER^{TAM};RIP7-Bcl-x$_L$* mice appear relatively benign, with clear boundaries between tumor and exocrine tissue (Figure 4A). Islets in comparably treated *pIns-MycER^{TAM};ARF$^{-/-}$* mice appear loculated with irregular boundaries with adjacent exocrine tissue, consistent with the extensive turnover and remodeling of the β cell compartment in such animals (Figure 4B). In contrast, 12 day β cell tumors in *pIns-MycER^{TAM};RIP7-Bcl-x$_L$;ARF$^{-/-}$* mice are massive, typically merging into large clusters with highly irregular boundaries from which invasive strands of β cells protrude far into the exocrine tissue (Figure 4C). β cell tumors in *p53$^{-/-}$* mice in which Myc had been activated for 12 days were similarly large, irregular, and invasive (Figure 4F). The large Myc-induced β cell tumors in both *pIns-MycER^{TAM};RIP7-Bcl-x$_L$;ARF$^{-/-}$* and *p53$^{-/-}$* mice were extensively infiltrated by tortuous and highly hemorrhagic vasculature (Figures 4D, 4G, 4J, and 4K). Still longer (21 day) sustained activation of Myc in *pIns-MycER^{TAM};RIP7-Bcl-x$_L$;ARF$^{-/-}$* mice drove progressive expansion and elaboration of the β cell tumors, leading to a dramatic hemorrhagic tumor phenotype (Figure 4E). Despite the overt similarities in overall rapid growth rate and general severity of β cell tumors in *pIns-MycER^{TAM};RIP7-Bcl-x$_L$;ARF$^{-/-}$* mice and p53-deficient animals, however, the two phenotypes remain distinct. Apoptosis is virtually absent from all Myc-induced tumors in *pIns-MycER^{TAM};RIP7-Bcl-x$_L$;ARF$^{-/-}$* mice but persists at appreciable levels in p53-deficient animals.

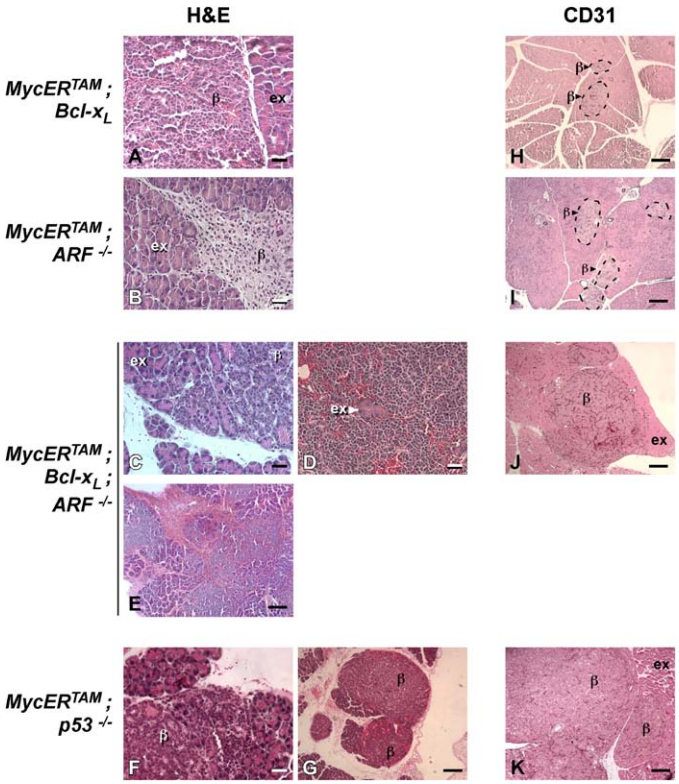

Figure 4. Myc-induced β cell tumors in *pIns-MycER^{TAM};RIP7-Bcl-x$_L$;ARF$^{-/-}$* and *pIns-MycER^{TAM};p53$^{-/-}$* are rapidly growing, aggressive, invasive, and angiogenic

Sections from 12 day (**A**–**D** and **F**–**K**) or 21 day (**E**) tumors of the indicated genotypes were stained with H&E (**A**–**G**) or anti-CD31 (**H**–**K**, in brown with eosin counterstain). Note the ragged edges of the islets from *pIns-MycER^{TAM};ARF$^{-/-}$* mice (**B**), indicating an invasive phenotype, despite lack of overall islet expansion. Myc-induced β cell tumors in *pIns-MycER^{TAM};RIP7-Bcl-x$_L$;ARF$^{-/-}$* mice have invasive and ragged margins (**C**) with extensive, tortuous, and hemorrhagic vasculature (**D** and **J**). After 21 days of sustained Myc activity in *pIns-MycER^{TAM};RIP7-Bcl-x$_L$;ARF$^{-/-}$* mice, β cell tumor mass occupies the majority of the pancreas (Figure 3L). Tumors in *pIns-MycER^{TAM};p53$^{-/-}$* mice are also highly invasive (**F**) with extensive and hemorrhagic angiogenesis (**G** and **K**). Examples of islets are indicated by "β" and exocrine pancreas by "ex." Scale bars are 20 μm (**A**–**D** and **F**) and 100 μm (**E** and **G**–**K**).

Discussion

Myc, like other dominant oncoproteins, triggers potent intrinsic tumor suppression pathways that curtail its otherwise powerful and pleiotropic oncogenic potential. Such tumor suppressor pathways in effect mask any immediate selective advantage that Myc activation would otherwise confer upon a somatic cell target (Lowe et al., 2004). As a consequence, Myc can drive oncogenesis only when such antagonistic pathways are either inactivated or sufficiently overwhelmed to allow net cell gain to prevail over cell loss. Apoptosis is the best-characterized intrinsic tumor suppressor pathway triggered by Myc, and several acute Myc activation models have demonstrated how suppression of apoptosis, either by antiapoptotic mutations such as overexpression of Bcl-2/Bcl-x$_L$ (Bissonnette et al., 1992; Fanidi et al., 1992; Pelengaris et al., 2002; Wagner et al., 1993) or through the action of survival signals (Harrington et al., 1994; Pelengaris et al., 1999), directly potentiates Myc's oncogenic function. The p19^{ARF}/p53 pathway is strongly implicated in the mediation of Myc-induced intrinsic tumor suppression pathways (reviewed in Evan and Vousden, 2001): loss of either p19^{ARF} or p53 greatly accelerates Myc oncogenesis in a wide variety of cell and tissue types, and selective loss of either p19^{ARF} or p53 is a common feature of Myc-induced tumors in several transgenic Myc mouse tumor models. However, since the p19^{ARF}/p53 pathway is capable of triggering either apoptosis or replicative arrest, depending upon cell type and circumstance, it has remained unclear which of these two discrete programs is the principal conduit of tumor suppression in any instance.

We compared the direct mechanisms by which Bcl-x$_L$ overexpression, ARF inactivation, and p53 loss each promote Myc's oncogenic function in vivo using an acutely switchable model of Myc oncogenesis targeted to pancreatic β cells. One of the major shortcomings of classical transgenic and knockout cancer models is that tumors arise sporadically and only after significant lag periods, implying that tumorigenesis requires additional, sporadic, and undefined oncogenic lesions. This is the case even when multiple cooperating mutations are combined and makes it impossible to assess whether the original lesions interact directly or indirectly, or by what mechanisms the cooperation arises. As is clear from evolutionary biology, acquisition of disadvantageous traits can, by constraining subsequent evolutionary trajectories, be every bit as influential in fostering success of eventual winners as acquisition of advantageous ones (Lenski et al., 2003). There is therefore no reason to assume that two mutations that together accelerate tumor formation necessarily confer any immediate selective advantage on the progenitor tumor cell in which they arise. In contrast to classical Myc transgenics, acutely switchable Myc models allow direct inspection, in real time, of the influence of ancillary

oncogenic lesions on both acute and sustained Myc action in target tissues residing in their orthotopic environments in vivo. Furthermore, because the pancreatic β cells harboring switchable Myc are distributed among hundreds of independent islet populations throughout the mouse pancreas, each *pIns-MycER^{TAM}* mouse is effectively several hundred independent, simultaneous tumorigenesis experiments. In the case of each of the cooperating lesions that we have investigated, Myc activation is sufficient to induce synchronous and rapid β cell tumorigenesis in essentially every one of the several hundred islets in the pancreas, indicating that no additional sporadic lesions are required. Such models therefore permit direct inspection, in real time, of the mechanism by which cooperating lesions modulate Myc's oncogenic potential at different stages of tumor growth in vivo.

Using our acutely switchable *pIns-MycER^{TAM}* β cell model, we demonstrate that, although Bcl-x_L overexpression, p19^{ARF} loss, and p53 inactivation all cooperate oncogenically with Myc, each lesion appears to cooperate by a distinct mechanism. In particular, whereas Bcl-x_L overexpression cooperates oncogenically with Myc by specifically blocking Myc-induced apoptosis, *ARF* loss cooperates by facilitating Myc-induced proliferation. The most dramatic consequence of this is that overexpression of Bcl-x_L and loss of p19^{ARF} themselves synergize with each other to dramatically potentiate the oncogenic potential of Myc relative to each alone. Interestingly, mere absence of p19^{ARF} is insufficient to allow Myc to drive widespread β cell expansion because the augmented proliferative capacity it affords is accompanied by a compensatory increase in apoptosis. Consequently, the only net consequence of Myc activation is that β cells in *ARF$^{-/-}$* islets turn over at a greatly enhanced rate compared with the ~60 day half-life of normal β cells (Bonner-Weir, 2000). Nonetheless, the balance between increased cell proliferation and cell death in *pIns-MycER^{TAM}/ARF$^{-/-}$* islets appears to be very finely poised since, on occasions, we have observed the occasional individual pancreatic islet to undergo significant Myc-induced expansion. We note with interest that the apoptotic response to Myc is actually increased in the absence of p19^{ARF}. Possibly this indicates that stresses associated with aberrant proliferation are the direct cause of apoptosis and that p19^{ARF}, by acting as a brake to such aberrant proliferation, serves to limit the apoptotic impact of Myc. That the same increase in apoptosis does not accompany p53 loss is presumably because p53, unlike p19^{ARF}, partakes directly in the cellular apoptotic response to aberrant proliferation through its direct links with the Puma/Noxa/Bax apoptotic machinery.

Overexpression of members of the antiapoptotic Bcl-2/Bcl-x_L protein family has been shown to suppress cell cycle entry in several cell types (Brady et al., 1996; Huang et al., 1997; O'Reilly et al., 1996) by a mechanism involving suppression of mitogenic E2Fs (Vairo et al., 2000). Since mitogenic E2Fs can be potent inducers of p19^{ARF}, we therefore considered the possibility that p19^{ARF} loss contributes to increased proliferation of Bcl-x_L-expressing β cells by abrogating Bcl-x_L-dependent suppression of β cell proliferation rather than by enhancing Myc-induced proliferation per se. While we cannot exclude the possibility that such additional interactions further enhance the synergy between Bcl-x_L overexpression and p19^{ARF} loss, the similarity in β cell proliferative indices in the *pIns-MycER^{TAM}* single versus the *pIns-MycER^{TAM};RIP7-Bcl-x_L* double transgenic islets following Myc activation suggests otherwise. Another conceivable mechanism by which p19^{ARF} loss could accentuate Myc-induced proliferation is suggested by recent observations that p19^{ARF} can directly interact with, and potentially inhibit, Myc's protein function (Datta et al., 2004; Qi et al., 2004). However, this would not explain why a similar enhancement of Myc's proliferative capacity is also observed in *p53$^{-/-}$* β cells that retain wild-type p19^{ARF} (Figure 1) or why it is that Myc-induced proliferation is inhibited by p19^{ARF} while Myc-dependent suppression of terminal differentiation is not (Figure 1).

Our previous studies using switchable Myc mouse tumor models demonstrated that, once apoptosis is abrogated, Myc instructs multiple aspects of the malignant phenotype, including cell growth, proliferation, dedifferentiation, tumor angiogenesis, and invasion (Pelengaris et al., 1999, 2002). It is therefore noteworthy that the extents of both angiogenesis and invasion, established hallmarks of more advanced tumorigenesis, correlate closely with the degree of Myc-induced proliferation we see in incipient Myc-induced tumors. Thus, the rapidly expanding Myc-induced tumors arising in the *pIns-MycER^{TAM};p53$^{-/-}$* and *pIns-MycER^{TAM};RIP7-Bcl-x_L;ARF$^{-/-}$* mice exhibit a far more severe invasive and angiogenic phenotype than those arising in *pIns-MycER^{TAM};RIP7-Bcl-x_L* animals.

Our data indicating that p19^{ARF} is irrelevant for mediating Myc-induced apoptosis would seem to be at odds with several elegant studies using Myc-driven lymphomagenesis models in the mouse. These have shown that suppression of apoptosis by Bcl-2 overexpression or Bax loss relieves pressure to inactivate the p53 pathway during tumor formation (Eischen et al., 2001; Schmitt et al., 2002), observations used to argue that the p19^{ARF}/p53 pathway is principally involved in mediating an apoptotic tumor suppressor program in response to Myc activation. There are several possible explanations for this apparent inconsistency. First, the situation in lymphoid cells may not be generally applicable to other cells types. Indeed, p53 activation is known to trigger apoptosis efficiently in lymphoid cells but in mesenchymal and many epithelial lineages, as in β cells, replicative arrest is a more common outcome, especially in vivo where abundant survival factors often exist to suppress apoptotic responses. Second, our data indicate that p19^{ARF} loss and p53 loss each exert a very different influence on Myc-induced apoptosis in vivo: while p53 loss confers some measure of protection from apoptosis, p19^{ARF} loss exacerbates it. Any functional prosurvival complementation between Bcl-2 overexpression and p53 loss is, therefore, unlikely to extend to loss of p19^{ARF}. More generally, loss of p19^{ARF} and loss of p53 seem unlikely to be equivalent since, even in the absence of p19^{ARF}, p53 can still be activated by a wide variety of stress signals that are likely to occur in developing tumors, including hypoxia and DNA damage. Conversely, increasing evidence points to p53-independent properties of p19^{ARF} (Kelly-Spratt et al., 2004; Kuo et al., 2003), in particular the induction of replicative arrest through its actions on ribosome biogenesis (Ayrault et al., 2004; Bertwistle et al., 2004; Sugimoto et al., 2003) and, as mentioned, the possible inhibition of Myc itself (Datta et al., 2004; Qi et al., 2004). Last, it is important to acknowledge that cancers kill because tumor burden, for whatever reason, becomes lethal. If either abrogation of apoptosis or loss of p53-induced growth suppression is each, alone, sufficient to allow outgrowth of a lethal Myc-induced tumor, then there would exist no significant evolutionary pressure to select for additional mutations in the other pathway before death of the organisms intervened.

Thus, while our data clearly indicate that combining Bcl-x_L overexpression and $p19^{ARF}$ loss confers dramatic additional selective advantages on incipient tumor cells, it remains to be seen how important their relative contributions are to naturally occurring tumors that arise over the extended timescales that mark human cancers.

Experimental procedures

Transgenic and knockout mice

Mice expressing $MycER^{TAM}$ under the control of the rat insulin promoter (*pIns-MycER^{TAM}*) (Pelengaris et al., 2002) were crossed with animals expressing Bcl-x_L under the same promoter (*RIP7-Bcl-x_L* mice [Zhou et al., 2000]) or onto an *ARF$^{-/-}$* (Kamijo et al., 1997) or *p53$^{-/-}$* (Donehower et al., 1992) background. $MycER^{TAM}$ was activated in β cells in situ by daily i.p. injection of Tamoxifen (1 mg/mouse/day) dissolved in peanut oil (Sigma). At least five mice were used in each experimental cohort, and reproducibility was extremely high, as described (Lawlor et al., 2006; Pelengaris et al., 2002). To identify cells in S phase, mice were injected i.p. with 2 μmol BrdU 3.5 hr prior to sacrifice. For histological analysis, pancreata were harvested, stored in Z-fix (Anatech Ltd, Battle Creek, MI) overnight, dehydrated, and embedded in paraffin, and 5 μm sections were prepared. Alternatively, pancreata were frozen in OCT compound (Sakura Finetek, Torrance, CA), and 10 μm sections were prepared. All studies involving animal subjects were performed in accordance with protocol number A10518-16702, approved by the UCSF IACUC.

Histology and immunofluorescence

Tissue sections (5 μm) were rehydrated and boiled in 10 mM sodium citrate (pH 6.0), for 5 min to recover antigens. Primary antibody (guinea pig anti-insulin [Linco], rat monoclonal anti-CD31 [BD Pharmingen], rabbit monoclonal anti-Ki67 [Neomarkers], rabbit polyclonals to $p19^{ARF}$ [Ab80; Abcam], p53 [CM5; Novocastra], ERα, and mouse monoclonal to $p21^{cip1}$ [BD Pharmingen]) was applied in blocking buffer (2.5% BSA, 5% goat serum, 0.3% Triton X-100 in PBS) for 2–16 hr. Incorporated BrdU and apoptotic cells were detected using a BrdU Detection kit II (Roche) and an Apoptag kit (Chemicon), respectively, according to the manufacturers' instructions. Secondary antibodies (from Dako and Molecular Probes) were applied in blocking buffer for 30 min. DAB development was accomplished using DAB reagents from Vector laboratories. Fluorescent antibody-labeled slides were rinsed in PBS and mounted in DAKO fluorescent mounting medium containing 1 μg/ml Hoechst. Fluorescence images were obtained in the Laboratory for Cell Analysis (UCSF Comprehensive Cancer Center) using a LSM510 confocal microscope (Zeiss) or an Axiovert 100 inverted microscope (Zeiss) equipped with a Hamamatsu Orca digital camera. Apoptosis and BrdU incorporation were quantified in tissue sections by counting randomized fields of islet cells and calculating the percentage of TUNEL- or BrdU-positive cells as a percentage of insulin-positive cells.

Determination of blood glucose

Mice were fasted for 4 hr, and 50 μl samples of blood were collected from the tail vein. Glucose levels were determined using Accu-Chek Active test strips (Roche Diagnostics Corp., Indianapolis, IN).

Acknowledgments

This work was supported by NIH grant RO1 CA98018, JDRF grant 4-2004-372, and funds from Daiichi Corp. to GIE and by NIH fellowship F32 CA106039 to K.S. We are most grateful to Fanya Rostker for her technical assistance and to our colleagues in the Evan lab for their invaluable criticism and advice.

Received: November 10, 2005
Revised: May 30, 2006
Accepted: June 22, 2006
Published: August 14, 2006

References

Adhikary, S., and Eilers, M. (2005). Transcriptional regulation and transformation by Myc proteins. Nat. Rev. Mol. Cell Biol. *6*, 635–645.

Ayrault, O., Andrique, L., Larsen, C.J., and Seite, P. (2004). Human ARF tumor suppressor specifically interacts with chromatin containing the promoter of rRNA genes. Oncogene *23*, 8097–8104.

Bertwistle, D., Sugimoto, M., and Sherr, C.J. (2004). Physical and functional interactions of the ARF tumor suppressor protein with nucleophosmin/B23. Mol. Cell. Biol. *24*, 985–996.

Bissonnette, R., Echeverri, F., Mahboubi, A., and Green, D. (1992). Apoptotic cell death induced by c-*myc* is inhibited by *bcl-2*. Nature *359*, 552–554.

Bonner-Weir, S. (2000). Life and death of the pancreatic beta cells. Trends Endocrinol. Metab. *11*, 375–378.

Brady, H.J., Gil-Gomez, G., Kirberg, J., and Berns, A.J. (1996). Bax alpha perturbs T cell development and affects cell cycle entry of T cells. EMBO J. *15*, 6991–7001.

Datta, A., Nag, A., Pan, W., Hay, N., Gartel, A.L., Colamonici, O., Mori, Y., and Raychaudhuri, P. (2004). Myc-ARF (alternate reading frame) interaction inhibits the functions of Myc. J. Biol. Chem. *279*, 36698–36707.

Donehower, L.A., Harvey, M., Slagle, B.L., McArthur, M.J., Montgomery, C.A., Jr., Butel, J.S., and Bradley, A. (1992). Mice deficient for p53 are developmentally normal but susceptible to spontaneous tumours. Nature *356*, 215–221.

Eischen, C.M., Weber, J.D., Roussel, M.F., Sherr, C.J., and Cleveland, J.L. (1999). Disruption of the ARF-Mdm2-p53 tumor suppressor pathway in Myc-induced lymphomagenesis. Genes Dev. *13*, 2658–2669.

Eischen, C.M., Roussel, M.F., Korsmeyer, S.J., and Cleveland, J.L. (2001). Bax loss impairs Myc-induced apoptosis and circumvents the selection of p53 mutations during Myc-mediated lymphomagenesis. Mol. Cell. Biol. *21*, 7653–7662.

Elson, A., Deng, C., Campos-Torres, J., Donehower, L.A., and Leder, P. (1995). The MMTV/c-myc transgene and p53 null alleles collaborate to induce T-cell lymphomas, but not mammary carcinomas in transgenic mice. Oncogene *11*, 181–190.

Evan, G.I., and Vousden, K.H. (2001). Proliferation, cell cycle and apoptosis in cancer. Nature *411*, 342–348.

Fanidi, A., Harrington, E.A., and Evan, G.I. (1992). Cooperative interaction between c-*myc* and *bcl-2* proto-oncogenes. Nature *359*, 554–556.

Harrington, E.A., Bennett, M.R., Fanidi, A., and Evan, G.I. (1994). c-Myc-induced apoptosis in fibroblasts is inhibited by specific cytokines. EMBO J. *13*, 3286–3295.

Hermeking, H., and Eick, D. (1994). Mediation of c-Myc-induced apoptosis by p53. Science *265*, 2091–2093.

Hsu, B., Marin, M.C., el-Naggar, A.K., Stephens, L.C., Brisbay, S., and McDonnell, T.J. (1995). Evidence that c-myc mediated apoptosis does not require wild-type p53 during lymphomagenesis. Oncogene *11*, 175–179.

Huang, D.C., O'Reilly, L.A., Strasser, A., and Cory, S. (1997). The anti-apoptosis function of Bcl-2 can be genetically separated from its inhibitory effect on cell cycle entry. EMBO J. *16*, 4628–4638.

Hurlin, P.J., and Dezfouli, S. (2004). Functions of Myc:Max in the control of cell proliferation and tumorigenesis. Int. Rev. Cytol. *238*, 183–226.

Juin, P., Hueber, A.O., Littlewood, T., and Evan, G. (1999). c-Myc-induced sensitization to apoptosis is mediated through cytochrome c release. Genes Dev. *13*, 1367–1381.

Kamijo, T., Zindy, F., Roussel, M.F., Quelle, D.E., Downing, J.R., Ashmun, R.A., Grosveld, G., and Sherr, C.J. (1997). Tumor suppression at the mouse INK4a locus mediated by the alternative reading frame product p19ARF. Cell *91*, 649–659.

Kamijo, T., Weber, J.D., Zambetti, G., Zindy, F., Roussel, M.F., and Sherr, C.J. (1998). Functional and physical interactions of the ARF tumor suppressor with p53 and Mdm2. Proc. Natl. Acad. Sci. USA *95*, 8292–8297.

Kelly-Spratt, K.S., Gurley, K.E., Yasui, Y., and Kemp, C.J. (2004). $p19^{ARF}$ suppresses growth, progression, and metastasis of Hras-driven carcinomas through p53-dependent and -independent pathways. PLoS Biol. *2*, E242. 10.1371/journal.pbio.0020242.

Kuo, M.L., Duncavage, E.J., Mathew, R., den Besten, W., Pei, D., Naeve, D., Yamamoto, T., Cheng, C., Sherr, C.J., and Roussel, M.F. (2003). Arf induces p53-dependent and -independent antiproliferative genes. Cancer Res. *63*, 1046–1053.

Lawlor, E., Soucek, L., Brown-Swigart, L., Shchors, K., Bialucha, C., and Evan, G. (2006). Reversible kinetic analysis of Myc targets *in vivo* provides novel insights into Myc-mediated tumorigenesis. Cancer Res., in press.

Laybutt, D.R., Weir, G.C., Kaneto, H., Lebet, J., Palmiter, R.D., Sharma, A., and Bonner-Weir, S. (2002). Overexpression of c-Myc in beta-cells of transgenic mice causes proliferation and apoptosis, downregulation of insulin gene expression, and diabetes. Diabetes *51*, 1793–1804.

Lenahan, M.K., and Ozer, H.L. (1996). Induction of c-myc mediated apoptosis in SV40-transformed rat fibroblasts. Oncogene *12*, 1847–1854.

Lenski, R.E., Ofria, C., Pennock, R.T., and Adami, C. (2003). The evolutionary origin of complex features. Nature *423*, 139–144.

Lowe, S.W., Cepero, E., and Evan, G. (2004). Intrinsic tumour suppression. Nature *432*, 307–315.

O'Reilly, L.A., Huang, D.C., and Strasser, A. (1996). The cell death inhibitor Bcl-2 and its homologues influence control of cell cycle entry. EMBO J. *15*, 6979–6990.

Pelengaris, S., Littlewood, T., Khan, M., Elia, G., and Evan, G. (1999). Reversible activation of c-Myc in skin: Induction of a complex neoplastic phenotype by a single oncogenic lesion. Mol. Cell *3*, 565–577.

Pelengaris, S., Khan, M., and Evan, G.I. (2002). Suppression of Myc-induced apoptosis in beta cells exposes multiple oncogenic properties of Myc and triggers carcinogenic progression. Cell *109*, 321–334.

Qi, Y., Gregory, M.A., Li, Z., Brousal, J.P., West, K., and Hann, S.R. (2004). p19(ARF) directly and differentially controls the functions of c-Myc independently of p53. Nature *431*, 712–717.

Schmitt, C.A., McCurrach, M.E., de Stanchina, E., Wallace-Brodeur, R.R., and Lowe, S.W. (1999). INK4a/ARF mutations accelerate lymphomagenesis and promote chemoresistance by disabling p53. Genes Dev. *13*, 2670–2677.

Schmitt, C.A., Fridman, J.S., Yang, M., Baranov, E., Hoffman, R.M., and Lowe, S.W. (2002). Dissecting p53 tumor suppressor functions in vivo. Cancer Cell *1*, 289–298.

Strasser, A., Harris, A.W., Bath, M.L., and Cory, S. (1990). Novel primitive lymphoid tumours induced in transgenic mice by cooperation between *myc* and *bcl*-2. Nature *348*, 331–333.

Sugimoto, M., Kuo, M.L., Roussel, M.F., and Sherr, C.J. (2003). Nucleolar Arf tumor suppressor inhibits ribosomal RNA processing. Mol. Cell *11*, 415–424.

Vairo, G., Soos, T.J., Upton, T.M., Zalvide, J., DeCaprio, J.A., Ewen, M.E., Koff, A., and Adams, J.M. (2000). Bcl-2 retards cell cycle entry through p27(Kip1), pRB relative p130, and altered E2F regulation. Mol. Cell. Biol. *20*, 4745–4753.

Wagner, A.J., Small, M.B., and Hay, N. (1993). Myc-mediated apoptosis is blocked by ectopic expression of *bcl*-2. Mol. Cell. Biol. *13*, 2432–2440.

Wagner, A.J., Kokontis, J.M., and Hay, N. (1994). Myc-mediated apoptosis requires wild-type p53 in a manner independent of cell cycle arrest and the ability of p53 to induce $p21^{waf1/cip1}$. Genes Dev. *8*, 2817–2830.

Zhou, Y.P., Pena, J.C., Roe, M.W., Mittal, A., Levisetti, M., Baldwin, A.C., Pugh, W., Ostrega, D., Ahmed, N., Bindokas, V.P., et al. (2000). Overexpression of Bcl-x(L) in beta-cells prevents cell death but impairs mitochondrial signal for insulin secretion. Am. J. Physiol. Endocrinol. Metab. *278*, E340–E351.

Zindy, F., Eischen, C.M., Randle, D.H., Kamijo, T., Cleveland, J.L., Sherr, C.J., and Roussel, M.F. (1998). Myc signaling via the ARF tumor suppressor regulates p53-dependent apoptosis and immortalization. Genes Dev. *12*, 2424–2433.